Z. Phys. B – Condensed Matter 86, 163–175 (1992)

Condensed Matter
Zeitschrift für Physik B

Original contributions

Screw dislocation mediated growth of sputtered and laser-ablated $YBa_2Cu_3O_{7-\delta}$ films

D.G. Schlom [1], D. Anselmetti [1,2], J.G. Bednorz [1], R.F. Broom [1], A. Catana [1], T. Frey [2]*, Ch. Gerber [1], H.-J. Güntherodt [2], H.P. Lang [2], and J. Mannhart [1]

[1] IBM Research Division, Zurich Research Laboratory, CH-8803 Rüschlikon, Switzerland
[2] Institute of Physics, University of Basel, Klingelbergstrasse 82, CH-4056 Basel, Switzerland

Received July 5, 1991

By imaging the as-grown surfaces of sputtered and laser-ablated $YBa_2Cu_3O_{7-\delta}$ films with scanning tunneling microscopy (STM), we have directly observed spiral-shaped growth terraces which emanate from screw dislocations. The density of screw dislocations was observed to decrease with increasing growth temperature and substrate misorientation. The surface structures observed by STM together with cross-sectional transmission electron microscope (TEM) images provide insights into the mechanisms of crystal growth operative during the formation of $YBa_2Cu_3O_{7-\delta}$ films grown using these two widespread techniques.

1. Introduction

Tremendous improvements in both bulk and thin-film forms of the cuprate superconductors have been brought about through greater understanding and control of their microstructure [1]. The majority of research conducted with the goal of understanding the growth mechanism and resulting growth morphology of $YBa_2Cu_3O_{7-\delta}$ thin films has been performed using TEM [2–4]. Recently, it has been demonstrated that high-quality images of the as-grown surfaces of $YBa_2Cu_3O_{7-\delta}$ films can be obtained by STM [5, 6]. Observations of sputtered [5, 6] and laser-ablated [7] $YBa_2Cu_3O_{7-\delta}$ films by STM have revealed the presence of high densities of screw dislocations ($\approx 10^9$ cm^{-2}), which not only are potentially strong vortex pinning sites [8], but also have a dramatic effect on film growth. The mechanism of introduction of such high dislocation densities into $YBa_2Cu_3O_{7-\delta}$ films is not yet understood and it is expected that control of the density of pinning sites, specifically dislocations, will be important for device applications of the high-T_c cuprates. In particular this may be vital for the highly anisotropic high-T_c cuprates containing Bi and Tl, since studies which considered solely point defect pinning sites concluded that these materials will not be useful for applications in high magnetic fields at 77 K [9, 10]. However, linear defects such as screw dislocations, capable of pinning a vortex along a substantial part of its length, may extend the temperature and magnetic field range in which these high-T_c cupreates may be utilized.

In this paper, after briefly describing the thin film preparation and measurement conditions, we report on the effect of substrate temperature and misorientation on the screw dislocation density. A decrease in dislocation density occurs as the substrate temperature is raised or the misorientation away from the substrate (100) plane is increased (for nominally (100) oriented substrates). Changes in the surface morphology of the films accompany the variation of these growth parameters, providing clues about the processes occurring during growth. The surface morphology of the laser-ablated $YBa_2Cu_3O_{7-\delta}$ films grown on various substrates is strikingly similar to that of the sputtered $YBa_2Cu_3O_{7-\delta}$ films, indicating that the same growth mode occurs in both of these widespread methods of thin film preparation. The STM and TEM morphological data are then discussed with respect to possible nucleation and growth mechanisms occurring in sputtered and laser-ablated $YBa_2Cu_3O_{7-\delta}$ films. Although these inferences are of a rather speculative nature it is hoped that the discussion of possible growth mechanisms together with the supporting evidence presented will stimulate additional studies.

2. Experimental

The $YBa_2Cu_3O_{7-\delta}$ films were grown by DC hollow cathode magnetron sputtering [11] and laser ablation [12]. Characteristics of the films to be discussed in this paper are listed in Table 1. The sputtered films were grown on undoped [13] and Nb-doped [14] $SrTiO_3$ (100) substrates. Colloidal silica was used for the final

* *Present address:* IBM T.J. Watson Research Center, Yorktown Heights, NY 10598, USA

Table 1. Growth conditions and properties of the samples investigated

Sample # [a]	Average thickness (nm)	Growth rate (nm/s)	T_{sub} (°C)	Screw Dislocation density at surface (10^8 cm^{-2})	Mis-orientation from (100): °→[011], °→[01$\bar{1}$]	T_c ($\rho=0$) (K)	J_c at 4.2 K (10^7 A/cm^2) (self-field)
S1 [b]	130	0.05	750	9.5±1.5	1.3, 0.6	89 [c]	4.7
S2a [d]	130	0.09	750	15.0±1	0, 0		
S2b [d]	130	0.09	750	5.5±1	1.4, 1.4	88 [c]	
S2c [d]	130	0.09	750	2.5±1	2, 0	88 [c]	
S2d [b]	130	0.09	750	0.7±0.3	3.5, 0.5	89 [c]	
S3 [b]	12	0.13	750	27.5±3	0.2, 0.1	82 [c]	
S4 [b]	60	0.13	750	14.5±2.5	0.7, 0.7	89 [c]	
S5 [b]	120	0.13	750	13.5±2	0.1, 0.1	88 [c]	6.0
S6 [b]	130	0.14	750	12.5±1	0.9, 0.7	88 [c]	3.2
S7 [b]	150	0.18	750	10.5±1	1.1, 0.8	89 [c]	6.5
S8 [b]	150	0.05	755	8.5±1	0.5, 0.3	89 [c]	6.9
S9 [b]	140	0.11	755	9.0±1	1.3, 0.1	84 [c]	3.1
S10 [b]	110	0.12	760	7.5±1	0.5, 0.3	87 [c]	4.4
S11 [b]	100	0.11	770	3.5±0.6	2.1, 0.6	86 [c]	1.6
S12 [b]	110	0.12	780	6.0±1	0.6, 0.5	87 [c]	1.8
S13 [b]	120	0.13	780	5.0±1	1.2, 0.2	87 [c]	
S14 [b]	130	0.14	780	0.5±0.2	2.2, 0.8	87 [c]	4.1
S15 [b]	100	0.11		13.5±1.5	0.8, 0.6	86 [c]	
L1a [b]	150	0.35	730	20.0±3		82 [e]	
L1b [f]	150	0.35	730	15.0±3		80 [e]	
L2 [b]	250	1.00	730	10.0±3		90 [e]	

[a] S refers to sputtered samples and L to laser-ablated samples
[b] $SrTiO_3$ substrate
[c] $\rho < 10^{-2} \rho_{100K}$
[d] Nb-doped (0.05%–0.3%) $SrTiO_3$ substrate
[e] Inductively measured
[f] MgO substrate

chem-mechanical polishing step in the in-house preparation of the latter substrates. Each substrate was rinsed in acetone and isopropanol, blown dry with nitrogen, and attached to the substrate heater block with silver paint. The sputtering conditions were: a sputtering pressure of 87 Pa ($Ar:O_2=2:1$), a plasma discharge of 150–180 V and 260–500 mA, and an after-growth cooldown in $\approx 5 \times 10^4$ Pa O_2 for about one hour. The temperature of the substrate heater block (T_{sub}) was measured with an optical pyrometer. The precision of the substrate temperature control employed is approximately ±10 °C.

The laser-ablated films were grown on $SrTiO_3$ (100) and MgO (100) substrates [15]. Each substrate was rinsed in acetone and propanol and attached to the substrate heater block with silver paint. Ablation took place with a KrF ($\lambda=248$ nm) excimer laser [16] radiating a $YBa_2Cu_3O_{7-\delta}$ target at an energy density of 2 J/cm^2 and a 3–10 Hz pulse rate in a growth chamber containing 27 Pa O_2. The target was rotated during deposition and polished to an optical smoothness between growth runs to minimize "boulders" in the laser-ablated films. After growth the samples were cooled in $\approx 3 \times 10^4$ Pa O_2 for 30 min to 450 °C, held at this temperature for half an hour, and then slowly cooled down to room temperature under flowing oxygen.

Critical current densities (J_c) were measured on bridges (8 μm × 100 μm) patterned using conventional photolithography and wet etching [8]. Electrical transport measurements on the sputtered films showed T_c ($\rho=0$) values typically between 87–89 K, resistivity ratios (ρ_{300}/ρ_{100}) of 2.5–3, and typical critical current densities $J_c=1$–8×10^6 A/cm^2 at 77 K and $J_c=1$–7×10^7 A/cm^2 at 4.2 K. Laser-ablated films grown using similar conditions to the films studied by STM had J_c values in the high 10^6 A/cm^2 to low 10^7 A/cm^2 range at 4.2 K.

The as-grown $YBa_2Cu_3O_{7-\delta}$ films were investigated by STM at room temperature in air using mechanically prepared $Pt_{0.80}Ir_{0.20}$ tips. No surface treatment was used prior to STM imaging. The use of a high tunneling resistance ($R_T > 3 \times 10^{10}$ Ω) was found to be crucial for attaining STM images without surface degradation [5]. A tunneling current (I_T) of about 300 pA and a tip bias voltage (V_T) of about 0.8 V were used for the laser-ablated films, while even lower values ($I_T=10$–20 pA and $V_T=0.5$–1 V) were used for the sputtered films. All of the images shown represent unfiltered raw data. The screw dislocation density was measured by averaging the number of growth centers in many images taken at different locations on the sample.

The STM results shown are characteristic of the many images taken of each sample (hundreds of images in all). Not only were different regions of each sample studied, but in many cases two samples cut from the same substrate and grown during the same sputtering run were examined. In these cases the surface morphology was indistinguishable for both samples, indicating that

the growth conditions were similar across the 20 mm × 20 mm region of the substrate heater block to which the samples were attached, thus allowing meaningful comparisons to be made [8] between the STM samples and the adjacently grown samples (from the same substrate) on which the critical current was measured.

The samples for TEM were prepared by standard cross section techniques [17]. All of the TEM images shown are cross-sectional. After mechanical dimpling, each specimen was ion milled to electron transparency. Liquid nitrogen cooling of the specimen was employed during the ion milling process in order to minimize damage to the specimen. The samples were viewed along the $SrTiO_3$ [010] zone axis in a JEOL 2010 microscope operating at 200 kV.

X-ray diffraction measurements showed that the *c*-axes of the sputtered $YBa_2Cu_3O_{7-\delta}$ films were oriented perpendicular to the substrate for $T_{sub} \gtrsim 750$ °C. For $T_{sub} \lesssim 750$ °C, *a*-axis growth normal to the substrate plane was also observed (i.e., mixed *a* and *c*). For this reason, all of the sputtered films in this study were initiated at $T_{sub} \gtrsim 750$ °C. X-ray diffraction revealed that the laser-ablated $YBa_2Cu_3O_{7-\delta}$ films were also *c*-axis oriented. The misorientation of the $SrTiO_3$ substrates from the nominal (100) orientation was determined by the Laue method with an accuracy of about $\pm 0.5°$.

In order to assign crystallographic directions to the STM images, the Laue method was used to determine the orientation of the in-plane axes of the $SrTiO_3$ substrate with respect to the sample position used for the STM observations. Although the in-plane epitaxial alignment between each $YBa_2Cu_3O_{7-\delta}$ film and $SrTiO_3$ substrate was not explicitly checked, based on previous studies [18–20] and TEM studies of some of these films, epitaxial alignment between the ⟨100⟩ axes of the $YBa_2Cu_3O_{7-\delta}$ films and the $SrTiO_3$ substrates was assumed. The ⟨100⟩ in-plane directions of the $YBa_2Cu_3O_{7-\delta}$ films are indicated in the STM images. No distinction between the [100] and [010] $YBa_2Cu_3O_{7-\delta}$ directions is made.

3. Results and discussion

3.1. Similarity between sputtered and laser-ablated $YBa_2Cu_3O_{7-\delta}$ films

The as-grown surface of a sputtered $YBa_2Cu_3O_{7-\delta}$ film on a $SrTiO_3$ (100) substrate is shown in Fig. 1. Growth spirals emanating from both left- and right-handed screw dislocations are clearly seen. Similar surface structures are seen in laser-ablated films grown on $SrTiO_3$ (100) and MgO (100) as shown in Fig. 2. The screw dislocations appear to be randomly distributed. The inherent similarity between the STM images of sputtered and laser-ablated $YBa_2Cu_3O_{7-\delta}$ films grown under conditions optimized with respect to transport properties, suggests that the same film growth mode is operative in both methods. Under alternate growth conditions (slightly lower substrate temperature) growth towers

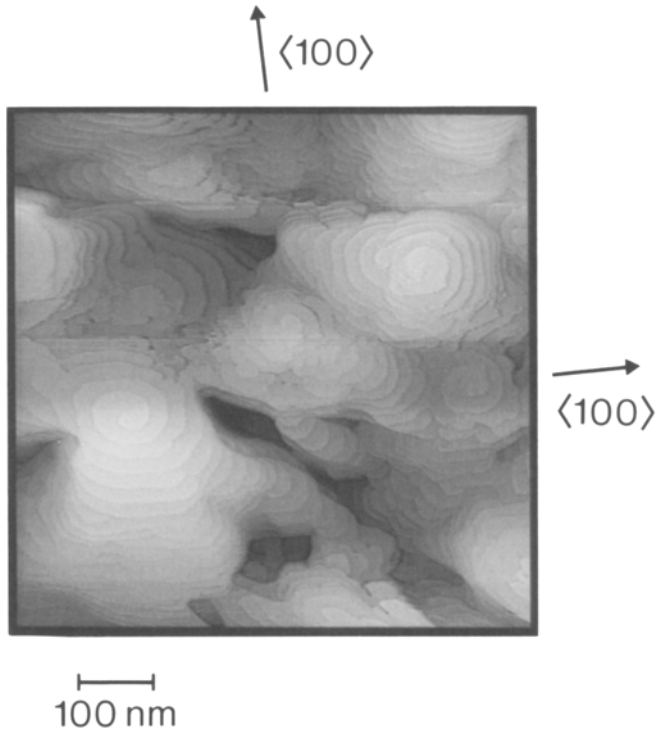

Fig. 1. STM image of a sputtered $YBa_2Cu_3O_{7-\delta}$ film grown on $SrTiO_3$ (100) (Sample S6) showing growth spirals emanating from both left- and right-handed screw dislocations. The in-plane ⟨100⟩ directions are indicated

each comprised of a stack of unit-cell-high layers, free of observable screw dislocations at their tops, have been observed in the laser-ablated films [21].

The steps between terraces of the growth spirals in the STM images are one unit cell high (about 1.2 nm), which indicates that these dislocations have a Burgers vector with a screw component normal to the surface of *c*[001].[1] In contrast to TEM observations of edge dislocations having Burgers vectors $\mathbf{b} = c[001]$ in which dissociation into three partial dislocations was observed [22], no dissociation of the screw dislocations (which would give rise to steps of fractional unit cell height) is seen in the STM images. Similar Burgers vectors have been identified by TEM in laser-ablated $YBa_2Cu_3O_{7-\delta}$ films [23]. This is in coinsiderable contrast to bulk samples, where a comparably high density of only *a*[001] or *b*[010] type Burgers vectors has been seen [24].

3.2. Microstructure observed by TEM

The STM observations which show a film surface roughness of about 10–20 nm and a high density of screw dislocations may initially seem inconsistent with the results of many TEM investigations that have been performed on $YBa_2Cu_3O_{7-\delta}$ films. In order to clarify whether our films are significantly different than or somehow consistent with those previously studied by

[1] Although we have not determined the total Burgers vector, we refer to these dislocations as though they are pure screw dislocations with Burgers vector, $\mathbf{b} = c[001]$

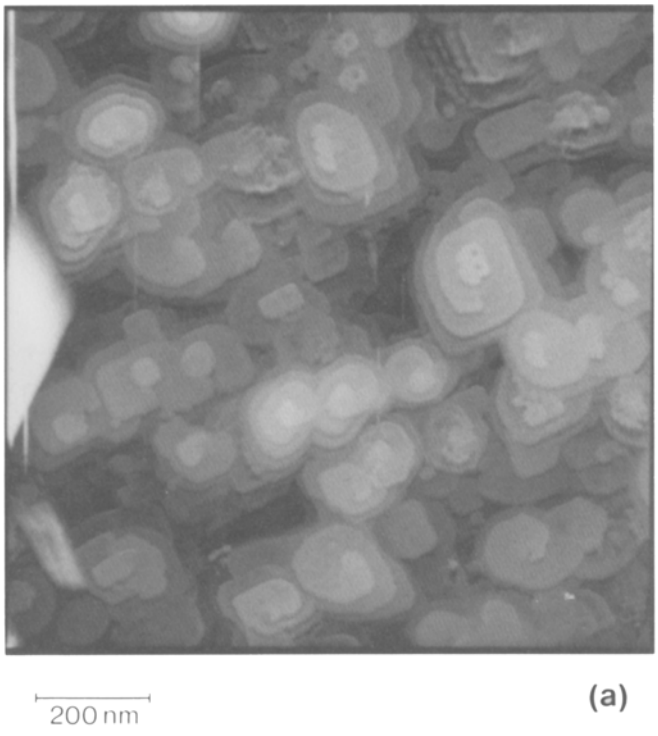

Fig. 2a, b. STM images of laser-ablated $YBa_2Cu_3O_{7-\delta}$ films grown on **a** $SrTiO_3$ (100) (Sample L1a) and **b** MgO (100) (Sample L1b) substrates

TEM, some of the same samples probed by STM were also examined using TEM.

Although extensive efforts were made to observe screw dislocations by TEM, such defects were not unequivocally identified. Rather, TEM images exhibiting

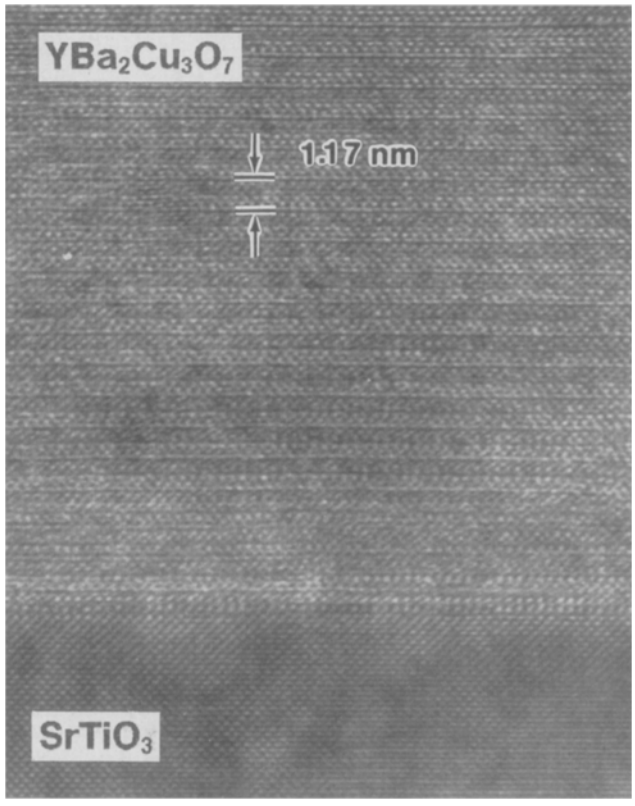

Fig. 3. A high resolution cross-sectional TEM image of a sputtered $YBa_2Cu_3O_{7-\delta}$ film showing the interface between the film and the $SrTiO_3$ (100) substrate (Sample S8)

well-ordered layering and epitaxial growth were observed, a typical example of which is shown in Fig. 3. The lack of observations of screw dislocations by bright field high-resolution TEM in $YBa_2Cu_3O_{7-\delta}$ films is not surprising considering that for threading screw dislocation densities of 10^9 cm^{-2}, in a cross-section thinned to 10 nm, on average only one dislocation would be present for every 10 μm of thinned region of specimen cross-section. Features of the surface morphology observed by STM were confirmed by TEM, as shown by the surface region of a sputtered $YBa_2Cu_3O_{7-\delta}$ film in Fig. 4. The roughness, both vertically, laterally, and in depth (as seen from the low magnification inset) in this thinned region of the TEM sample is consistent with the surface morphology revealed by STM (see Fig. 1). Further, the (001) layers on the right side of the image are slightly inclined with respect to those on the left side, which would be consistent with a slice through a growth spiral (Fig. 4). If this were the case the slope of the (001) planes would be greatest closest to the screw dislocation core. This is in agreement with the TEM image where the more tilted (001) planes lie beneath the highest region of the surface.

These films contain a high density of defects, as exemplified by the dark field TEM image shown in Fig. 5. Here, the entire height of the film is contained between the interface with the substrate and the upper surface. The surface morphology, due to a superposition through the larger depth of the sample, appears flatter than in TEM images of thinner regions or in STM images. Fur-

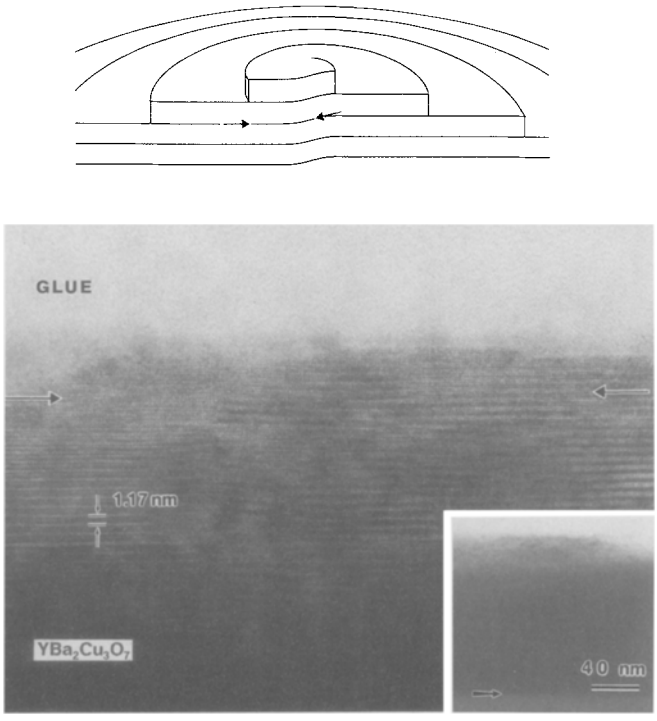

Fig. 4. A cross-sectional TEM image of the surface region of a sputtered $YBa_2Cu_3O_{7-\delta}$ film (Sample S8). The roughness is consistent with that revealed by STM (Fig. 10). The layers on the right side of the image (the thickest part of the sample) are slightly tilted with respect to those on the left side. Arrows paralleling each set of planes are shown. As sketched in an exaggerated manner in the schematic (above the TEM photo), the observed inclination between the two sets of (001) planes is consistent with a cross-sectional slice through a growth spiral. The inset shows a lower magnification view of this same region in which the entire film height, including the interface with the $SrTiO_3$ (100) substrate (at the arrow), may be seen. This TEM sample is thinner than that shown in Fig. 5, and correspondingly displays greater roughness

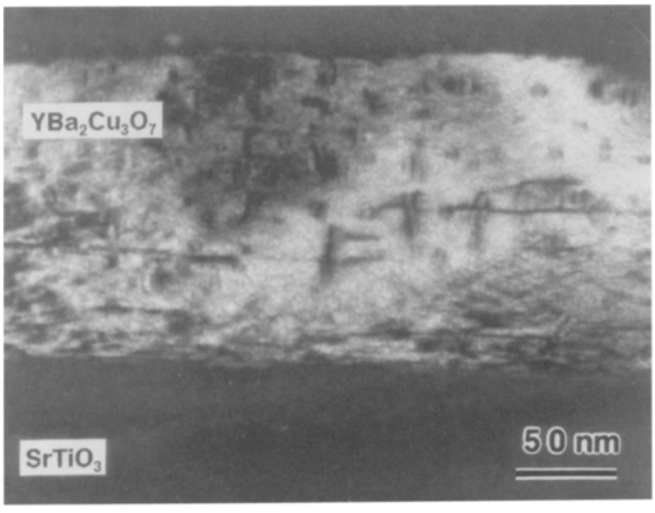

Fig. 5. A dark field TEM image ($\mathbf{g}=(010)$) of a sputtered $YBa_2Cu_3O_{7-\delta}$ film showing the entire film thickness (Sample S8)

ther details of the TEM microstructure of these sputtered films will appear elsewhere [25].

The microstructure observed by TEM on other sputtered [26] and laser-ablated [27] $YBa_2Cu_3O_{7-\delta}$ films is consistent with the STM and TEM microstructure seen in our films. For example, a TEM image in the publication by Eom et al. [26] (Fig. 10 in Ref. 26) shows thickness extrema in the region where threading defects meet the surface of the sputtered $YBa_2Cu_3O_{7-\delta}$ film. Also, threading dislocation densities of $\approx 10^9$ cm^{-2} were observed in laser-ablated films by Eibl et al. [27] (Fig. 4 in Ref. 27).

3.3. Effect of growth conditions on screw dislocation density

Growth temperature, growth rate [5], and substrate misorientation have an effect on the screw dislocation density. Figure 6 shows STM images of films grown at T_{sub} = 750, 760, 770, and 780 °C on $SrTiO_3$ (100) substrates. The trend of decreasing screw dislocation density with increasing substrate temperature is shown in Fig. 7.

These nominally (100) oriented $SrTiO_3$ substrates showed considerable variation (up to 2.3° off) in surface orientation. Measurements of the misorientation indicated that at a fixed temperature the dislocation density decreased with increasing misorientation, thus explaining some of the scatter in Fig. 7.

In order to corroborate this trend directly, four samples of differing misorientation were grown side by side during the same sputtering run. Three of the samples were deposited on Nb-doped $SrTiO_3$ substrates oriented and polished with chosen misorientation; the fourth was deposited on a misoriented $SrTiO_3$ substrate supplied by the same vendor as the others used in this study [13] in order to check that the doping and alternate surface preparation of the doped substrates was not a dominant factor in the morphological changes accompanying misorientation. STM images of such a Nb-doped bare substrate indicated a roughness of about 2 nm.

One Nb-doped $SrTiO_3$ substrate was oriented to (100) (±0.5°), one was misoriented by 2° toward the [011] direction, and one was misoriented by 2° toward the [010] direction. The commercial $SrTiO_3$ substrate was misoriented mainly in the [011] direction. These misorientations were chosen based on previous studies of $YBa_2Cu_3O_{7-\delta}$ films grown on vicinal $SrTiO_3$ (100) substrates [28]. TEM investigations of annealed bare $SrTiO_3$ (100) have revealed the presence of steps whose edges are parallel to the ⟨010⟩ and ⟨011⟩ in-plane directions [29]. The latter orientation of step edges is believed to be responsible for the preferred alignment of twin boundaries in $YBa_2Cu_3O_{7-\delta}$ films grown on vicinal $SrTiO_3$ (100) substrates [28], where a dominance of (011) twin boundaries over (01$\bar{1}$) twin boundaries for substrates misoriented toward [011] was found.

STM images of films grown on these substrates of chosen orientation are shown in Fig. 8. Note that the ⟨100⟩ faceted terraces of the $YBa_2Cu_3O_{7-\delta}$ film are consistently stepped along the [011] direction of misorientation of the $SrTiO_3$ substrates. This same morphology is observed in the films grown at $T_{sub} \gtrsim 770$ °C in Fig. 6. Further, the surface screw dislocation density is observed to decrease as the misorientation angle increases for vi-

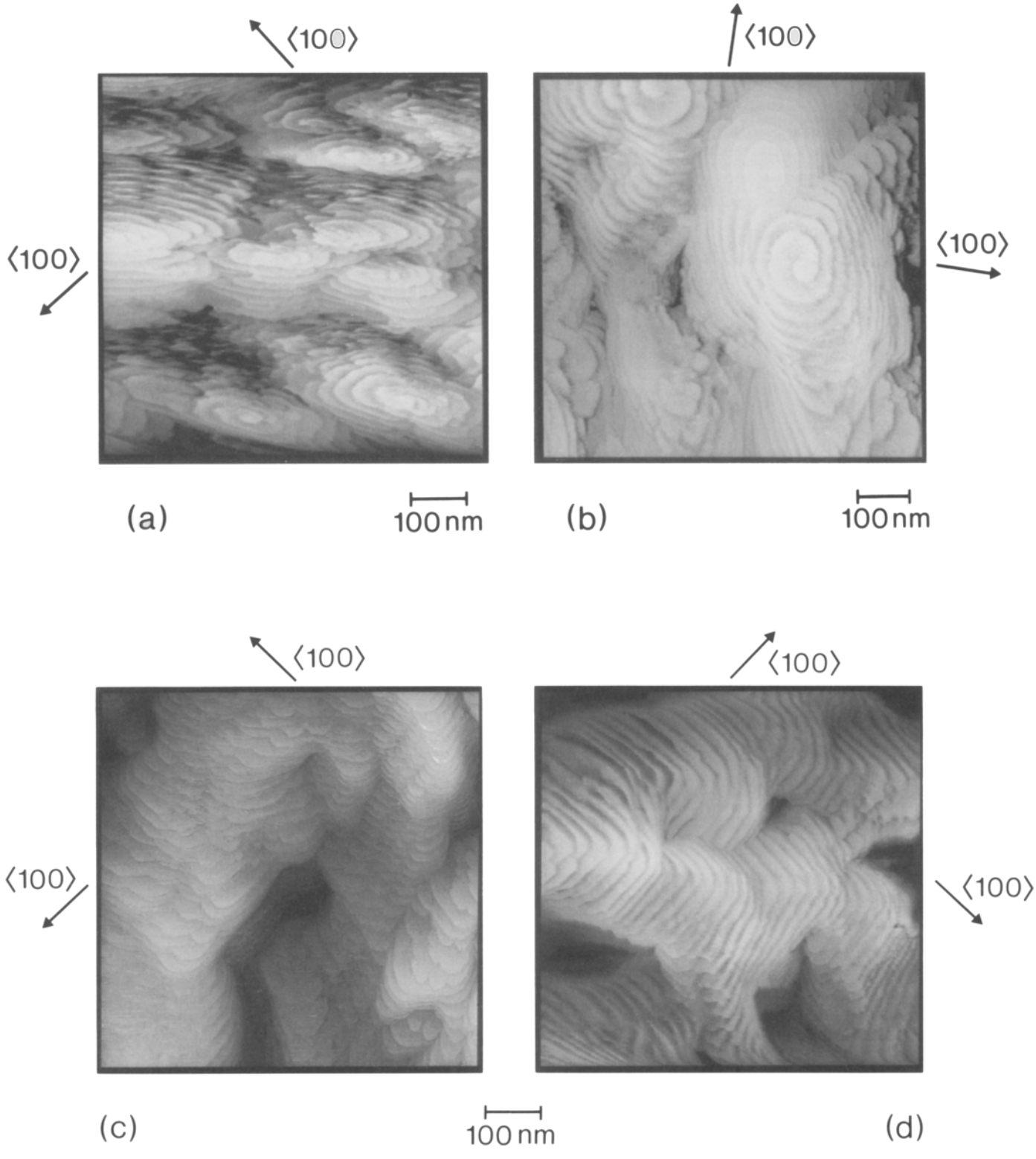

Fig. 6a–d. STM images of sputtered $YBa_2Cu_3O_{7-\delta}$ films grown at **a** $T_{sub} \approx 750$ °C (Sample S5), **b** $T_{sub} \approx 760$ °C (Sample S10), **c** $T_{sub} \approx 770$ °C (Sample S11), and **d** $T_{sub} \approx 780$ °C (Sample S14). The in-plane ⟨100⟩ directions are indicated

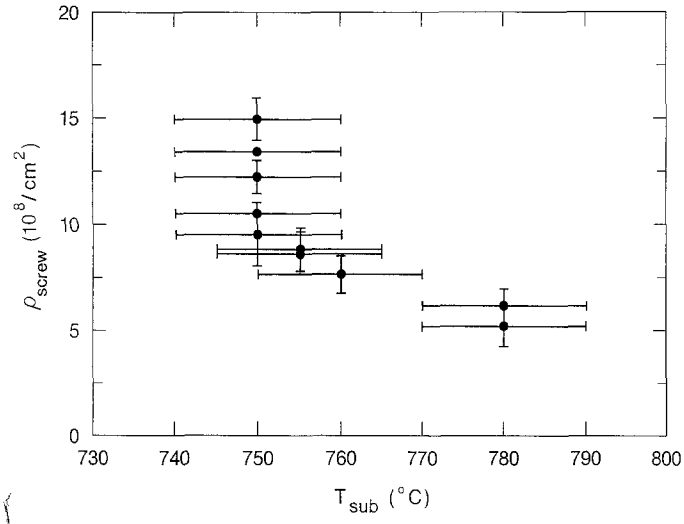

Fig. 7. Measured screw dislocation density as a function of growth temperature for 100–150 nm thick films sputtered on nominally (100) oriented $SrTiO_3$ substrates (misorientation $<2°$) at growth rates ranging from 0.05–0.18 nm/s

cinal $SrTiO_3$ (100) surfaces. This trend is plotted in Fig. 9 for all the samples grown at $T_{sub} = 750$ °C. Thus, growth rate [5], growth temperature, and substrate orientation are all important parameters for controlling the density of screw dislocations.

Although the STM images reveal that the $YBa_2Cu_3O_{7-\delta}$ films grown on $SrTiO_3$ substrates misoriented away from (100) are smoother on a nanometer scale than those grown on well-oriented $SrTiO_3$ (100) substrates, interestingly, an *increase* in surface roughness with height differences approaching the entire film thickness was observed on a micrometer scale by scanning electron microscopy (SEM) and TEM [25].

3.4. Nanometer-size holes

In Figs. 1 and 10 many (of the order of 10^{10} cm^{-2}) dark spots (each about 5–10 nm across) can be seen, which are either holes more than 2 nm deep or are due to insulating regions which may accompany significant atomic displacements known to occur within a ≈ 1 nm diameter core surrounding edge dislocations [30]. The latter possibility is less likely because changes in the tunneling behavior of the STM tip, due to tip damage which accompanies scanning over such insulating regions, were not observed. The growth fronts frequently envelop these spots, as though these spots impede the crystal growth process. This implies that the spots denote entities present during growth and are not due to tip-induced damage occurring during STM imaging. If these spots are indeed holes, their depth implies that at least one terrace has moved over them without filling them in. The presence of incipient edge dislocations having large[2] Burgers vectors at the center of these holes would explain the presence of such holes, why the holes appear to impede the film growth process, and why the holes propagate from layer to layer. STM images of laser-ablated $YBa_2Cu_3O_{7-\delta}$ films also show the presence of holes which are tens of angstroms deep [7, 21]. TEM investigations have revealed incipient dislocations in holes in thin (≈ 6 nm) $YBa_2Cu_3O_{7-\delta}$ films and tubular voids in thick (200–300 nm) $YBa_2Cu_3O_{7-\delta}$ films grown on MgO (100) substrates [2]. The Burgers vector of the screw dislocations present in these sputtered and laser-ablated $YBa_2Cu_3O_{7-\delta}$ films may also be sufficiently large to produce a hole at its core, which should be observable by STM at atomic resolution. Atomic resolution of dislocation-free regions of $YBa_2Cu_3O_{7-\delta}$ surfaces was recently achieved by STM [7].

3.5. Screw dislocation mediated growth

Although the growth spirals appear as isolated islands or hillocks separate from one another, use of the phrase "island growth" to describe this microstructure might be confused with established terminology used for the classification of thin film growth modes. Bauer [34] introduced three classifications for film growth: layer-by-layer growth (Frank-van der Merwe), initial layer growth followed by island growth (Stranski-Krastanov), and island growth (Volmer-Weber). These classifications are based on the relative surface energies of the substrate and overlayer, and the strain energy in the overlayer [35]. One of these growth modes should characterize a particular substrate/overlayer system independent of film preparation technique in the absence of surface defect sites. Defect sites, however, such as screw dislocations, are known to impact the crystal growth process greatly by supplying low-energy positions for adatom incorporation [36–39]. Since the STM images do not indicate which of these classical growth modes would be operative in the *absence* of the screw dislocations, we use the term "screw dislocation mediated growth" to describe the growth mechanism leading to the observed microstructure, for the film thickness range investigated (i.e. $\gtrsim 12$ nm).[3] This well-known [36–39] growth mechanism involves the addition of adatoms to the surface step which is always present along the edge of each spiral-shaped growth terrace emanating from a screw dislocation.

In previous studies on laser-ablated films [2], it was concluded that the growth mechanism is island growth, due to the observation of $YBa_2Cu_3O_{7-\delta}$ islands nucleating along the surface steps of the MgO substrate. But as others have pointed out [3], nucleation at existing steps on the substrate does not necessarily indicate an islands growth mechanism. Steps on the substrate surface and the continual growth step present around a screw dislocation are both low energy attachment sites; these are preferred attachment sites regardless of the mode of crystal growth [39]. The regularly spaced steps present on vicinal substrates are readily seen to impact

[2] According to Frank's approximate theory [31] the smallest Burgers vector having an energetically stable hollow core in isotropic materials lies in the range $|\mathbf{b}|_{min} = 20\pi\gamma/\mu$ to $40\pi\gamma/\sqrt{e}/\mu$. Frank estimated that typically $|\mathbf{b}|_{min}$ must be larger than the order of 10 Å [31]. Using the values of the surface energy ($\gamma = 1.6$ J/m^2) [32] and shear modulus ($\mu = 59$ GPa) [33] of $YBa_2Ba_3O_{7-\delta}$, this formula yields $|\mathbf{b}|_{min} = 1.7$–5.6 nm

[3] The film thicknesses given throughout this paper are average thicknesses

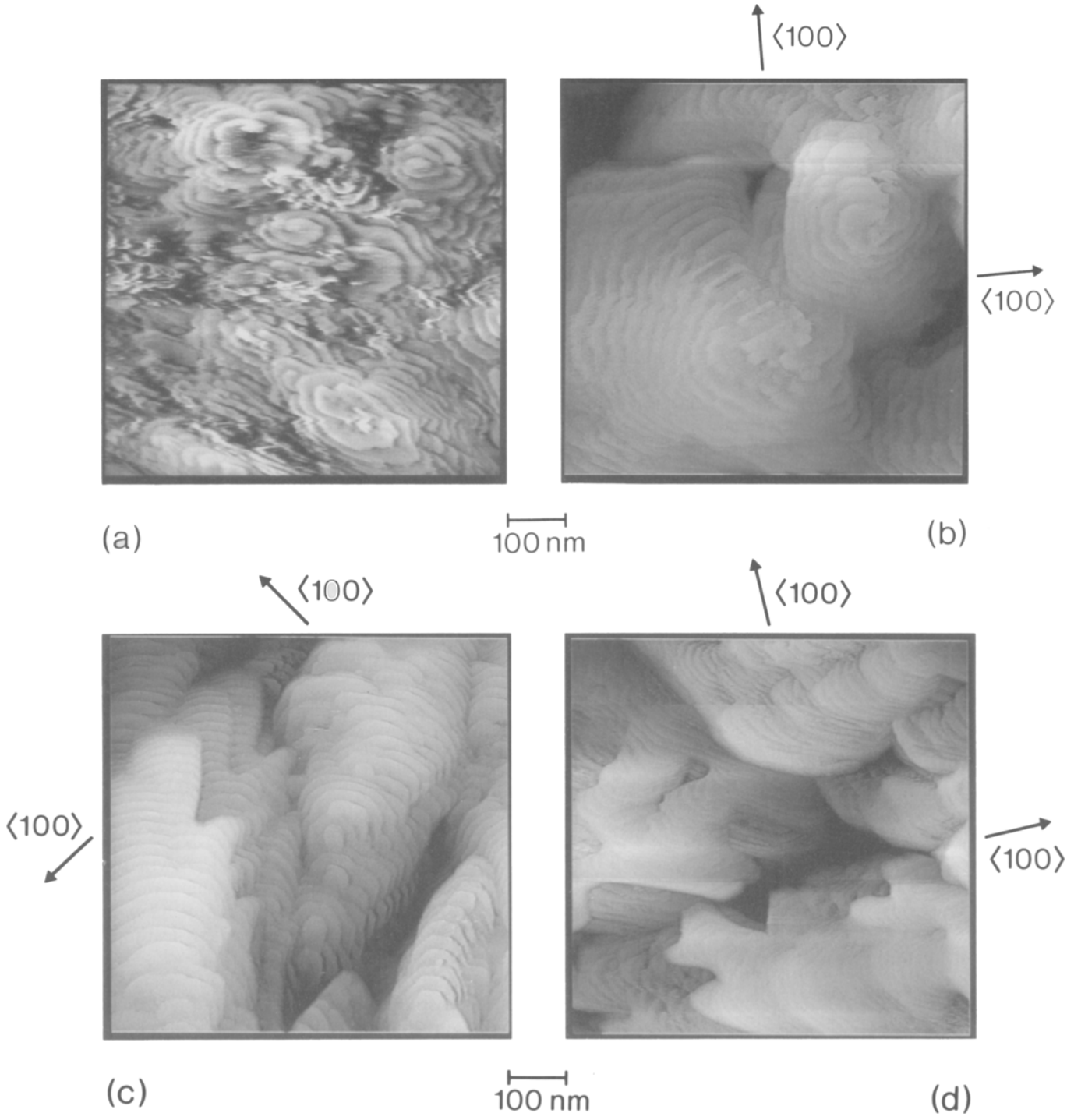

Fig. 8a–d. STM images of sputtered $YBa_2Cu_3O_{7-\delta}$ films grown during the same growth run on vicinal Nb-doped $SrTiO_3$ (100) substrates misoriented by **a** 0° (Sample S2a), **b** 2° → [010] (Sample S2b), **c** 2° → [011] (Sample S2c), and **d** an undoped $SrTiO_3$ (100) misoriented by 3.5° → [011] and 0.5° → [0$\bar{1}$1] (Sample S2d). The in-plane ⟨100⟩ directions are indicated

the growth mode as is evident from the stepped morphology seen in Figs. 6c, 6d, 8b, 8c, and 8d. This implies that growth occurs mainly by step propagation on vicinal $SrTiO_3$ (100) surfaces.

In many of the STM images a residue of irregular shape is seen at the edges of growth steps. Clumps of material (as seen in Fig. 10) or regions appearing to be at significantly lower height [6] are frequently seen. Whether these regions are really nanometers lower in height is not possible to ascertain from these constant current STM images, where the apparent height is a function of both the true height and the surface electronic characteristics. The residue at the step edges (the growth front) may be the remnants of a phase out of which crystallization occurred.

The shape of the growth spirals is consistent with

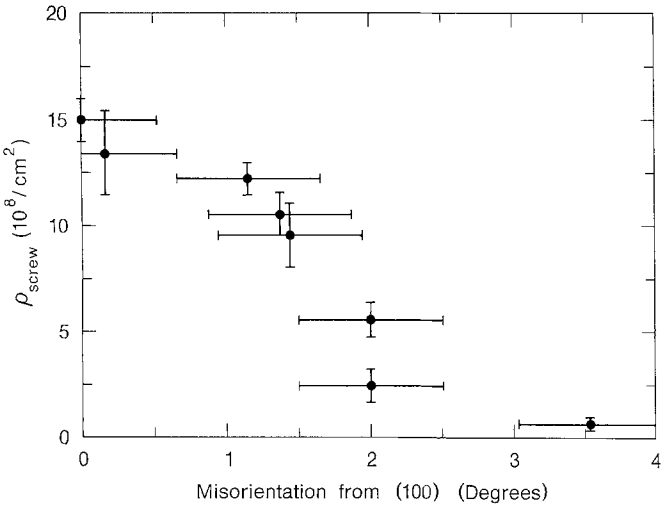

Fig. 9. Measured screw dislocation density as a function of substrate misorientation angle for 100–150 nm thick sputtered $YBa_2Cu_3O_{7-\delta}$ films grown at $T_{sub} \approx 750$ °C and 0.05–0.18 nm/s on Nb-doped and undoped nominally (100) oriented $SrTiO_3$ substrates

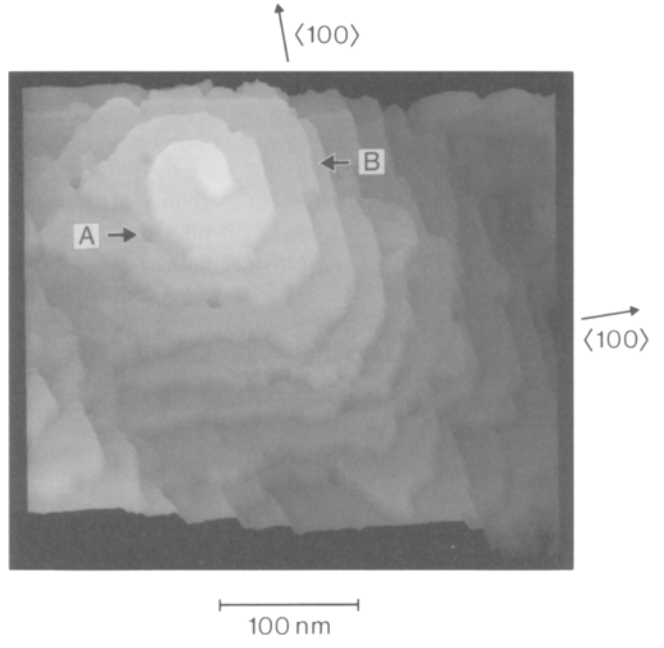

Fig. 10. STM image of a sputtered $YBa_2Cu_3O_{7-\delta}$ film (Sample S8). The small dark spots such as the one at arrow A are holes or isolated insulating regions. Clumps of material with irregular shape, for example at arrow B, are present at the step edges. The in-plane ⟨100⟩ directions are indicated

screw dislocation mediated growth theory [37, 40]. A circular growth spiral is expected when the surface diffusion length greatly exceeds the distance between kink sites for all edges of the growing step, independent of their crystallographic orientation. However, the distance between kink sites depends on crystallographic orientation: kinks are farther apart on more closely packed habit faces than on high index planes [40]. Thus, as the growth temperature is lowered, faceting of the growth spiral is expected to occur. The corners of a faceted growth spiral are constrained by the fact that the radius of curvature of every part of a growth spiral must exceed the radius of curvature of the corresponding part of the two-dimensional critical nucleus in order for growth to occur [37, 40]. Yet as the temperature is lowered, the corners of the critical nucleus become less rounded, independent of supersaturation [37]. All of these effects suggest that the spirals should become more faceted with decreasing growth temperature.

Indeed, the observed growth spirals are not perfectly round but exhibit growth temperature-dependent faceting on their {100} edges. Faceting on these faces is expected since the {100} and (001) planes are the observed habit faces of bulk $YBa_2Cu_3O_{7-\delta}$ crystals [42]. To test directly temperature-dependent faceting of the growth spirals, the growth of a sputtered $YBa_2Cu_3O_{7-\delta}$ film was initiated at $T_{sub} = 760$ °C (the first ≈ 15 nm) and then T_{sub} was lowered to 700 °C for the duration of growth (an additional ≈ 85 nm). X-ray diffraction data indicated that this film consisted mainly of grains with their *c*-axes oriented perpendicular to the substrate, and a minority with their *a*-axes oriented normal to the substrate. The concentration of *a*-axis perpendicular grains was significantly less than for samples grown entirely at $T_{sub} = 700$ °C. An STM image of the surface of this film is shown in Fig. 11. The growth spirals are far more faceted than their counterparts grown at a higher substrate temperature (see for example, Fig. 7). The observation of more faceted growth spirals for sputtered $YBa_2Cu_3O_{7-\delta}$ films grown on MgO (100) substrates compared with those grown on $SrTiO_3$ (100) substrates [6] is consistent

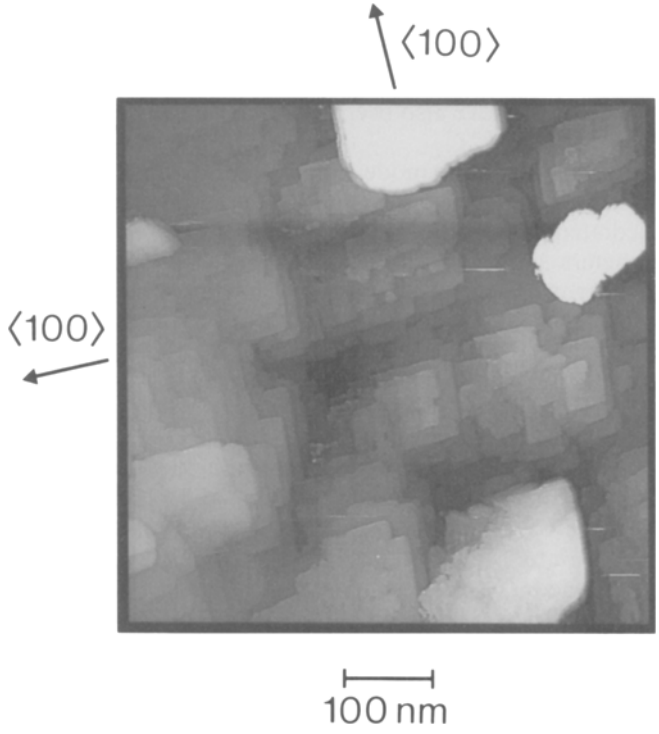

Fig. 11. STM image of a sputtered $YBa_2Cu_3O_{7-\delta}$ film (Sample S15). The growth was initiated at $T_{sub} \approx 760$ °C, but after the growth of about 15 nm the substrate block temperature was lowered to ≈ 700 °C for the duration of the growth. The in-plane ⟨100⟩ directions are indicated

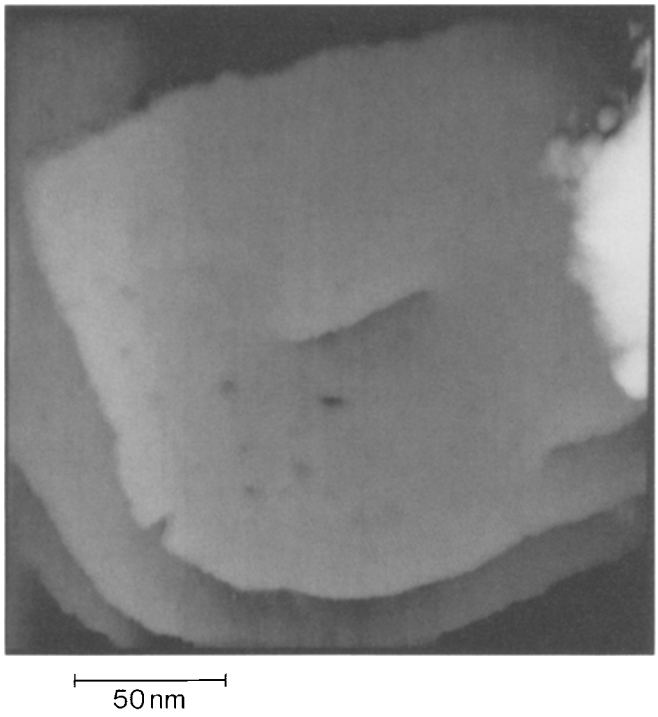

Fig. 12. STM image of a laser-ablated $YBa_2Cu_3O_{7-\delta}$ film showing an isolated step present between a pair of screw dislocations of opposite sign (Sample L2)

with the lower deposition temperatures used for growth on MgO.

Another expectation of screw dislocation mediated growth theory [36, 37] is that pairs of oppositely signed screw dislocations in close proximity generate loops during growth, the stacking of which forms a tower rather than a spiral. Such a dislocation pair is shown in Fig. 12. Similar pairs have also been seen in $HoBa_2Cu_3O_{7-\delta}$ thin films by STM [21].

Based on simple models of crystal bonding, diffusion, and the driving force of crystallization, screw dislocation mediated growth theory specifies measurable growth parameters such as the spacing between successive turns of a growth spiral, the rate of growth spiral rotation, and the total rate of growth [37, 40]. By measuring these parameters for complex growth systems, such as the growth of $YBa_2Cu_3O_{7-\delta}$ by sputtering, parameters of the simple growth model appropriate to the complex system can be determined. For example, for the distance $d = 20 \pm 6$ nm between successive turns of a growth spiral far from the stress field of the central screw dislocation,[4] we have been able to calculate the diffusion coefficient appropriate to the standard growth models. Screw dislocation mediated growth theory [41] states that the diffusion coefficient D is given by:

$$D \approx \frac{k_B T_{sub} v_{growth} d^2}{17.2 \gamma h a_{jump}^2} \quad (1)$$

[4] These measurements were made over a hundred nanometers away from the center of the growth spiral. From the measured value of $d \approx 20$ nm, the radius of influence of the dislocation stress field [41] $r_{stress} \approx 0.038[(\mu b^2 d)/\gamma]^{1/2}$ was calculated to be 1.2 nm using a shear modulus $\mu = 59$ GPa [33], Burgers vector length $b = 1.17$ nm, and surface energy $\gamma = 1.6$ J/m^2 [32]

where k_B is Boltzman's constant, T_{sub} is the growth temperature, v_{growth} is the macroscopic growth rate, γ is the surface energy per unit area at the step edge, h is the step height, and a_{jump} is the diffusion jump length. Inserting the values $T_{sub} \approx 1023$ K, $v_{growth} \approx 0.1$ nm/s, $d \approx 20$ nm, $\gamma^{\{100\}} \approx 1.6$ J/m^2 (Ref. 32), $h = |\mathbf{b}| = 1.17$ nm, and $a_{jump} \approx (abc)^{1/3} = [(0.382)(0.389)(1.17)]^{1/3}$ nm into Eq. (1) yields $D \approx 5 \times 10^{-16}$ cm^{-2}/s for the growth of $YBa_2Cu_3O_{7-\delta}$ films by sputtering at 750 °C. This diffusion coefficient encompasses all of the diffusion processes occurring during growth: from the surface diffusion of the constituents to their eventual accomodation into the growing crystal.

3.6. *Generation of screw dislocations*

The mechanism leading to the generation of high densities of screw dislocations in sputtered and laser-ablated $YBa_2Cu_3O_{7-\delta}$ thin films may lead to the controlled introduction of these defects. Possible dislocation introduction mechanisms include inheritance from the substrate, generation by the formation of dislocation half-loops, or by the incoherent meeting of growth fronts [43]. Inheritance from the substrate may be ruled out since the dislocation density of the substrates is several orders of magnitude lower than the $\approx 10^9$ cm^{-2} screw dislocations observed in these films. For $SrTiO_3$ substrates this has been demonstrated by both etch pit methods [5, 44] as well as Rutherford backscattering spectrometry (RBS) analysis [45]. Stacking faults are know to be quite common in $YBa_2Cu_3O_{7-\delta}$ films prepared by sputtering and laser ablation, and structural edge dislocations with Burgers vector $\mathbf{b} = c[001]$ have been observed in laser-ablated films by TEM [23]. A stacking fault or impurity phase inclusion could give rise to a dislocation half-loop which contains a pure edge segment parallel to the plane of the substrate and which intersects the surface of the film as two screw dislocations of opposite sign. However, the TEM images of these films do not show a high density of dislocation half-loops, indicating that this is not the mechanism of screw dislocation production either. The incoherent meeting of growth fronts has been observed to produce screw dislocations which then act as growth centers in the growth of synthetic micas [46]. An analogous process may occur in these $YBa_2Cu_3O_{7-\delta}$ films in the initial stages of growth.

This process, one of several screw dislocation generation mechanisms described by Baronnet [46], involves the dividing of an advancing growth front into two branches by an obstacle (e.g., an impurity). These branches continue to grow and eventually meet up with each other. In the case where the growth front is advancing in the horizontal plane, when the two branches meet and recombine with an offset in their vertical positions and their horizontal axes aligned, a screw dislocation is produced. In the case of a vertical offset and recombination of the branches with non-aligned horizontal axes, a twist boundary will exist at the interface between the recombined branches and further growth will not be favored.

This generation mechanism is favorable for layered substances which are capable of flowing over irregularities (giving rise to the vertical misalignment when the branches reunite) while retaining their crystalline structure. Synthetic micas are clearly able to grow this way [46]. TEM images of $YBa_2Cu_3O_{7-\delta}$ films reveal that they are also capable of bending over surface irregularities on the substrate [3, 27].

In the growth of $YBa_2Cu_3O_{7-\delta}$ films, screw dislocations may be generated during the initial stages of substrate coverage and island coalescence by a generation mechanism analogous to that observed in micas [46]. TEM images [26, 27] indicate that a high density of threading defects, including dislocations, are generated in the vicinity of the substrate. STM studies of thin ($\approx$12 nm) sputtered $YBa_2Cu_3O_{7-\delta}$ films on $SrTiO_3$ (100) substrates indicated a slightly higher surface screw dislocation density compared to thicker films (up to 150 nm), but with notably fewer turns in their associated growth spirals [5] (Fig. 13). In thick films, growth spirals having up to 20 turns were imaged [5]. The fact that these spirals are just beginning to develop as growth centers might imply that the screw dislocations are generated at about the same time that the coverage of the substrate is completed. Further, the dislocation density of the film with faceted growth spirals shown in Fig. 11 is comparable to that of films grown at $T_{sub}=760$ °C, even though the majority of film growth occurred at $T_{sub}=700$ °C. This result may seem surprising considering the higher dislocation density that would be expected from Fig. 7. However, this observation is consistent with the suggestion that the screw dislocations are generated during the process of island coalescence, and that the temperature during island coalescence is a determining factor in dislocation generation.

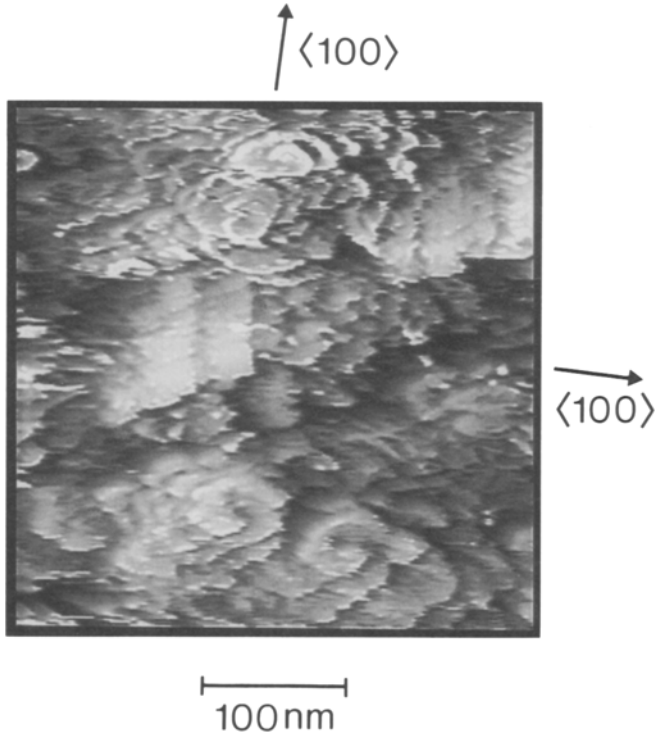

Fig. 13. STM image of a 12 nm thick sputtered $YBa_2Cu_3O_{7-\delta}$ film (Sample S3)

3.7. Defect generation during growth spiral coalescence

The coalescence of nuclei that occurs during the initial stages of growth on a foreign substrate surface not perfectly lattice-matched to the deposited overlayer is known to result in the generation of dislocations due to rotational or translational misalignment of the coalescing nuclei [43, 47]. For example, 10^{11} dislocations/cm^2 were observed in the coalescence of $YBa_2Cu_3O_{7-\delta}$ nuclei on MgO substrates in the early stages of sputtered film growth [3]. In an analogous manner, during screw dislocation-mediated growth, misalignments of impinging terraces of growth spirals may also occur leading to the generation of defects [6]. These defects include not only dislocations and point defects acting to accommodate in-plane misalignments of the coalescing terraces, but if the joining terraces are offset from each other along the *c*-axis, an out-of-phase domain may occur when they unite.

These various defects at the periphery of the growth spirals, which presumably are correlated with the screw dislocation density, are further potential vortex pinning sites. The implied vortex pinning structure consists of pinning at screw dislocation cores, each of which is encompassed by a number of accompanying pinning centers.

3.8. Layer-by-layer growth

A fundamentally different growth mode, layer-by-layer growth, has been inferred for the growth of ultrathin (<15 nm) $YBa_2Cu_3O_{7-\delta}$ films by *e*-beam coevaporation [48]. The observation of reflection high-energy electron diffraction (RHEED) intensity oscillations during the *e*-beam coevaporation $YBa_2Cu_3O_{7-\delta}$ films [48] is attributed to a cyclic process consisting of layer nucleation followed by layer filling, occurring as each unit cell high layer grows (a layer-by-layer or multilayer growth process). For this process to occur, the surface diffusion length must be shorter than the distance between existing growth steps (e.g., those due to the presence of screw dislocation-induced growth spirals), and thus would not be expected to occur for screw dislocation mediated growth. On the other hand, thicker (120 nm) $YBa_2Cu_3O_{7-\delta}$ films grown by thermal coevaporation contain a high density (over 10^{10} cm^{-2}) of screw dislocations [49].

4. Conclusions

The inherent similarity between the surface morphology of laser-ablated and sputtered $YBa_2Cu_3O_{7-\delta}$ films indicates that for the growth conditions employed the same growth mode is operative in both methods of thin film preparation. The high density of growth spirals ($\approx 10^9$ cm^{-2}) revealed by STM in films grown by these

two techniques indicates that the growth of these films occurs by a screw dislocation-mediated mechanism. Our observations are compatible with a screw dislocation generation mechanism involving the incoherent reunion of growth fronts during the process of islands of coalescence [46]. TEM images of these films are consistent both with the surface morphology revealed by STM images and with the TEM images of other groups, indicating that the defect microstructure revealed by STM is a general feature of these preparation techniques. Growth parameters have been found which strongly influence the screw dislocation density: an increasing screw dislocation density accompanies increasing growth rate [5], while increasing growth temperature or substrate misorientation cause a decrease in screw dislocation density. These growth parameters can be used to control the dislocation density of sputtered and laser-ablated $YBa_2Cu_3O_{7-\delta}$ films for specific applications [50]. This ability is of particular importance for the fabrication of heterostructures such as superlattices and tunnel junctions.

The authors gratefully acknowledge fruitful interactions with K.A. Müller, B. Koslowski for developing STM capabilities vital to this work, stimulating discussions with D.R. Clarke, R.F. Cook, U. Dürig and S.K. Streiffer, support from the Laser Science and Technology Department of the IBM Zurich Research Laboratory, and the technical assistance of D. Widmer.

References

1. See for example, Advances in superconductivity III: Proceedings of the 3rd International Symposium on Superconductivity. Berlin, Heidelberg, New York: Springer 1991
2. Norton, M.G., Carter, C.B.: J. Cryst. Growth **110**, 641 (1991)
3. Streiffer, S.K., Lairson, B.M., Eom, C.B., Clemens, B.M., Bravman, J.C., Geballe, T.H.: Phys. Rev. B **43**, 13007 (1991)
4. Ramesh, R., Chang, C.C., Ravi, T.S., Hwang, D.M., Inam, A., Xi, X.X., Li, Q., Wu, X.D., Venkatesan, T.: Appl. Phys. Lett. **57**, 1064 (1990)
5. Gerber, Ch., Anselmetti, D., Bednorz, J.G., Mannhart, J., Schlom, D.G.: Nature **350**, 279 (1991)
6. Hawley, M., Raistrick, I.D., Beery, J.G., Houlton, R.J.: Science **251**, 1587 (1991)
7. Lang, H.P., Frey, T., Güntherodt, H.-J.: Europhys. Lett. **15**, 667 (1991)
8. Mannhart, J., Anselmetti, D., Bednorz, J.G., Catana, A., Gerber, Ch., Müller, K.A., Schlom, D.G.: Z. Phys. B – Condensed Matter **86**, 177 (1992)
9. Palstra, T.T.M., Batlogg, B., van Dover, R.B., Schneemeyer, L.F., Waszczak, J.V.: Phys. Rev. B **41**, 6621 (1990)
10. Palstra, T.T.M., Batlogg, B., Schneemeyer, L.F., Waszczak, J.V.: Phys. Rev. B **43**, 3756 (1991)
11. Xi, X.X., Linker, G., Meyer, O., Nold, E., Obst, B., Ratzel, F., Smithey, R., Strehlau, B., Weschenfelder, F., Geerk, J.: Z. Phys. B – Condensed Matter **74**, 13 (1989)
12. Dijkkamp, D., Venkatesan, T., Wu, X.D., Shaheen, S.A., Jisrawi, N., Min-Lee, Y.H., McLean, W.L., Croft, M.: Appl. Phys. Lett. **51**, 619 (1987)
13. Commercial Crystal Laboratories, Inc. (Naples, Florida)
14. Binnig, G., Baratoff, A., Hoenig, H.E., Bednorz, J.G.: Phys. Rev. Lett. **45**, 1352 (1980)
15. Societé d'Equipement Industriel (La Tour du pin, France)
16. Lambda Physik LPX 300i (Göttingen, Germany)
17. Bravman, J.C., Sinclair, R.: J. Electron Microsc. Tech. **1**, 53 (1984)
18. Meyer, O., Weschfelder, F., Geerk, J., Li, H.C., Xiong, G.C.: Phys. Rev. B **37**, 9757 (1988)
19. Hwang, D.M., Venkatesan, T., Chang, C.C., Nazar, L., Wu, X.D., Inam, A., Hegde, M.S.: Appl. Phys. Lett. **54**, 1702 (1989)
20. Chaudhari, P., LeGoues, F.K., Segmüller, A.: Science **238**, 342 (1987)
21. Lang, H.P., Frey, T., Sum, R., Güntherodt, H.-J.: (Proceedings of the E-MRS Conference, Strasbourg, 1991) J. Less-Comm. Met. (to be published)
22. Chisholm, M.F., Smith, D.A.: Philos. Mag. A **59**, 181 (1989)
23. Ramesh, R., Hwang, D.M., Barner, J.B., Nazar, L., Ravi, T.S., Inam, A., Dutta, B., Wu, X.D., Venkatesan, T.: J. Mater. Res. **5**, 704 (1990)
24. Nakahara, S., Jin, S., Sherwood, R.C., Tiefel, T.H.: Appl. Phys. Lett. **54**, 1926 (1989)
25. Catana, A. et al.: (in preparation)
26. Eom, C.B., Sun, J.Z., Lairson, B.M., Streiffer, S.K., Marshall, A.F., Yamamoto, K., Anlage, S.M., Bravman, J.C., Geballe, T.H., Laderman, S.S., Taber, R.C., Jacowitz, R.D.: Physica C **171**, 354 (1990)
27. Eibl, O., Roas, B.: J. Mater. Res. **5**, 2620 (1990)
28. Budai, J.D., Chisholm, M.F., Feenstra, R., Lowndes, D.H., Norton, D.P., Boatner, L.A., Christen, D.K.: Appl. Phys. Lett. **58**, 2174 (1991)
29. Norton, M.G., Summerfelt, S.R., Carter, C.B.: Appl. Phys. Lett. **56**, 2246 (1990)
30. Gao, Y., Merkle, K.L., Bai, G., Chang, H.L.M., Lam, D.J.: Physica C **174**, 1 (1991)
31. Frank, F.C.: Acta Crystallogr. **4**, 497 (1951)
32. Cook, R.F., Dinger, T.R., Clarke, D.R.: Appl. Phys. Lett. **51**, 454 (1987). The surface energy ($\gamma = 1.6$ J/m^2) was calculated using the formulas and indentation crack length measurements given in this reference together with the value of Young's modulus ($E = 151$ GPa) from Ref. 33. These indentation crack length measurements and the inferred surface energy are for {100}-type planes. The surface energy of (001) planes are likely lower (as discussed in this reference), which would result in a lower value of $|\mathbf{b}|_{\min}$. Of course, a proper treatment of calculating $|\mathbf{b}|_{\min}$ requires an extension of Frank's theory to anisotropic materials
33. Ledbetter, H., Lei, M.: J. Mater. Res. (submitted for publication)
34. Bauer, E.: Z. Kristallogr. **110**, 372 (1958)
35. Bauer, E., Poppa, H.: Thin Solid Films **12**, 167 (1972)
36. Frank, F.C.: Disc. Farad. Soc. **5**, 48 (1949)
37. Burton, W.K., Cabrera, N., Frank, F.C.: Philos. Trans. R. Soc. London Ser. A **243**, 299 (1951)
38. Mutaftschiev, B.: In: Dislocations in solids. Nabarro, F.R.N. (ed.), Vol. 5, p. 57. Amsterdam: North-Holland 1980
39. Venables, J.A., Spiller, G.D.T., Hanbücken, M.: Rep. Prog. Phys. **47**, 399 (1984)
40. Frank, F.C.: Adv. Phys. **1**, 91 (1952)
41. Dürig, U., Bilgram, J.H., Känzig, W.: Phys. Rev. A **30**, 946 (1984). See equations 6.1, 6.11, 6.13, and 6.14
42. Kaiser, D.L., Holtzberg, F., Chisholm, M.F., Worthington, T.K.: J. Cryst. Growth **85**, 593 (1987). Faceting of $YBa_2Cu_3O_{7-\delta}$ nuclei along {100} planes and to a lesser extent along {110} planes has been observed by plan-view TEM (Ref. 3)
43. Pashley, D.W.: In: Thin films. p. 59. Metals Park: American Society for Metals 1964
44. Bednorz, J.G., Scheel, H.J.: J. Cryst. Growth **41**, 5 (1977)
45. Meyer, O., Weschenfelder, F., Xi, X.X., Xiong, G.C., Linker, G., Geerk, J.: Nucl. Instrum. & Methods B**35**, 292 (1988). Furthermore, these researchers suggested that high densities of dislocations were present in sputtered $YBa_2Cu_3O_{7-\delta}$ films based on the energy dependence of the dechanneling yield of their RBS measurements
46. Baronnet, A.: J. Cryst. Growth **19**, 193 (1973)
47. Epitaxial growth. Matthews, J.W. (ed.), Part B. New York: Academic Press 1975
48. Terashima, T., Bando, Y., Iijima, K., Yamamoto, K., Hirata, K., Hayashi, K., Kamigaki, K., Terauchi, H.: Phys. Rev. Lett. **65**, 2684 (1990)

49. Baudenbacher, F., Hirata, K., Berberich, P., Kinder, H., Assmann, W., Lang, H.P.: (Proceedings of the M^2S-HTSC III, Kanazawa, 1991) Physica C (to be published)
50. Mannhart, J., Bednorz, J.G., Müller, K.A., Schlom, D.G.: Z. Phys. B – Condensed Matter **83**, 307 (1991)
51. Burger, J., Bauer, P., Veith, M., Saemann-Ischenko, G.: Proceedings STM '91. International Conference on Scanning Tunneling Microscopy, Interlaken,Switzerland, August 12–16, 1991. Ultramicroscopy (to be published)
52. Yue, A.S.: Private communication
53. Maggio-Aprile, I., Kent, A.D., Niedermann, Ph., Renner, Ch., Antognazza, L., Miéville, L., Brunner, O., Triscone, J.-M., Fischer, Ø.: Proceedings STM '91. International Conference on Scanning Tunneling Microscopy, Interlaken, Switzerland, August 12–16, 1991. Ultramicroscopy (to be published)
54. Sun, B.N., Taylor, K.N.R., Hunter, B., Matthews, D.N., Ashby, S., Sealey, K.: J. Cryst. Growth **108**, 473 (1991)

Note added in proof. Since submitting this paper, the observation of growth spirals emanating from screw dislocations has been reported for $YBa_2Cu_3O_{7-\delta}$ films grown by a wide variety of growth techniques, such as thermal coevaporation [49], chemical vapor deposition (CVD) [51], liquid phase epitaxy (LPE) [52], and planar DC magnetron sputtering [53], in addition to the off-axis DC magnetron sputtering and laser ablation reported herein. Much larger growth spirals are also seen on bulk $YBa_2Cu_3O_{7-\delta}$ single crystals [54]. Thus, it appears that screw dislocations are a general feature of $YBa_2Cu_3O_{7-\delta}$ growth for a wide range of growth conditions.